Available online at www.sciencedirect.com
SCIENCE DIRECT®
Applied Surface Science 208–209 (2003) 210–217
applied surface science
www.elsevier.com/locate/apsusc

Microstructural study of CO_2 laser machined heat affected zone of 2024 aluminum alloy

D. Araújo[a,*], F.J. Carpio[a], D. Méndez[a], A.J. García[a], M.P. Villar[a], R. García[a], D. Jiménez[b], L. Rubio[b]

[a]*Departamento de Ciencia de los Materiales e Ingeniería Metalúrgica y Química Inorgánica, Universidad de Cádiz, 11510 Puerto Real, Cádiz, Spain*
[b]*EADS-CASA, Avda Marconi 33, 11011 Cádiz, Spain*

Abstract

Laser machining is an attractive alternative to traditional machining of Al 2024 because critical operation parameters in aeronautic industry like processing time, versatility, contamination and finish can be improved. The main disadvantage of laser machining is the high temperatures reached by the studied material during the laser processing. A heat affected zone (HAZ) extension lower than 5 μm is observed. The microstructural analysis shows that this HAZ suffers a heating between 548 and 596 °C where α-liquid phases are present. The high N_2 gas pressure used for the laser cutting induces three types of roughness on this viscous material during the laser processing. To improve this feature, the use of other laser wavelengths and/or power is proposed. The higher quality of the process can also be reached using other aeronautic materials with lower Cu content as 7475 Al alloy.

PACS: 42.62.C; 61.72.M; 81.40.G

Keywords: Laser machining; Aluminum 2024 T3; Microstructure

1. Introduction

Laser technology is planned to be used in aeronautic operations due to plenty advantages, such as the short processing time required, its possibility to be coupled to robotic arms and to the clean processing in term of acoustic and dust.

Due to the high number of drilling and cutting processes needed for aeroplane building, robotization of laser technology can give high benefits. Thus, the use of lasers is proposed as an alternative to traditional drilling and machining [1].

Among the aeronautic materials, Al alloys are one of the most promising for laser machining implantation, despite its very low absorption (∼1% room temperature, 7.7% melt) [2]. Al–Zn–Mg alloys are restricted for laser machining due to their environmental sensitive fracture in service [3]. This can be improved by the addition of Cu (7475 alloy [4] or 2xxx series) but Cu is also known to degrade the laser cutting quality. Even though, laser processing has been shown to improve the fatigue resistance in case of superficial treatment (laser shock peening, LSP) of pure aluminum as a result of the increased dislocation

* Corresponding author. Tel.: +349-56016351; fax: +349-56016288.
E-mail address: daniel.araujo@uca.es (D. Araújo).

0169-4332/02/$ – see front matter
doi:10.1016/S0169-4332(02)01375-2

density, and the decrease of surface roughness and compressive residual stress [5–7]. For the case of machining, the material reaches a high temperature that should modify this behavior as well as thermal conductivity and physical changes [8]. In addition, the effects of the high temperatures reached during the processing and the high reflectivity of the Al at the CO_2 laser wavelength ($\lambda \cong 10$ μm) make it unsuitable up to now for aeronautic certification.

In this paper, the microstructural changes of the heat affected zone of laser machined Al 2024 T3 have been analyzed after fatigue test and related to macroscopic properties to carry out aeronautic requirements and quality specifications.

First, an experimental study design is presented; second, optical and scanning electron microscopy micrographs are analyzed to understand the mechanisms involved in the laser machining of Al 2024. Finally, implications of such mechanisms on mechanical properties are analyzed.

2. Experimental

The studied samples are aluminum 2024 sheets with the following nominal composition: $Al_{94}Cu_{4.4}Mg_{1.5}$. Theses samples were thermally treated according to T3 treatment, which consists in solution immersion, cold wrought hardening and natural aging. Sample dimensions are 330 mm × 40 mm × 1.6 mm, (standard aeronautic fatigue test samples) with an orbital drilled using 2 kW continuous CO_2 laser to produce a 8 mm diameter hole as shown in Fig. 1.

To study the crack formation fatigue tests were performed and stopped just when the crack propagation began. Tests were carried out on a Suzpecar MUF-20 fatigue tester coupled to Suzpecar software (Version F-105) for data acquisition. The HAZ of the samples are studied in cross-section, in the case of broken samples, and in plan view, for non-broken samples, both by optical microscopy (OM) and scanning electron microscopy (SEM).

For the microstructural characterization of grain boundaries, the phases and the precipitates are revealed by Keller wet etching after the sanding and polishing. Compositional studies are also carried out by X-ray dispersive energy (EDX) coupled to SEM.

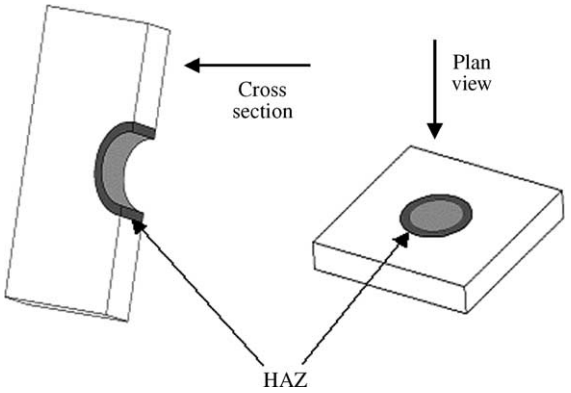

Fig. 1. Sample observation orientation respect to the laser orbital cut hole with its respective heat affected zone (HAZ). The cross-section where mechanically cut in the center of the hole to study the HAZ vs. the laser processing depth.

3. Results

The first feature is the increasing thickness of the HAZ when the laser optical power decreases (Fig. 2a). Indeed the deeper the hole is, the lower the power becomes and the thicker is the HAZ. Note also that liquid material can drip pushed by the gas pressure making thicker the HAZ, in the bottom part of the sample. The grains are shown to be elongated in the direction perpendicular to the machined surface as a result of the laminate process performed during the material manufacturing. The darker superficial contrasts correspond to a partially melted zone (labeled HAZ). The arrow labeled as A indicates the laser beam entrance and arrow B the bottom surface of the sample where the laser beam comes out. In this region shown by arrow C the material drips out of the orbitally machined hole as a result of the N_2 gas pressure. This indicates that during laser processing, the material first is heated in its solid state, and then becomes a mixture of α-liquid above 580 °C. At this point, the laser absorption changes from 1 to 8% [8] inducing the evaporation/sublimation of the liquid and α phases, respectively. Direct sublimation from low temperature solid state does not occur as demonstrated by the dripped material. Moreover, Fig. 2b shows that the grain structure persists in the α-liquid region demonstrating that the material does not completely reach the liquid phase (follow arrows). This means that this region remains below 650 °C being directly evaporated/sublimated (liquid/a phases, respectively). This

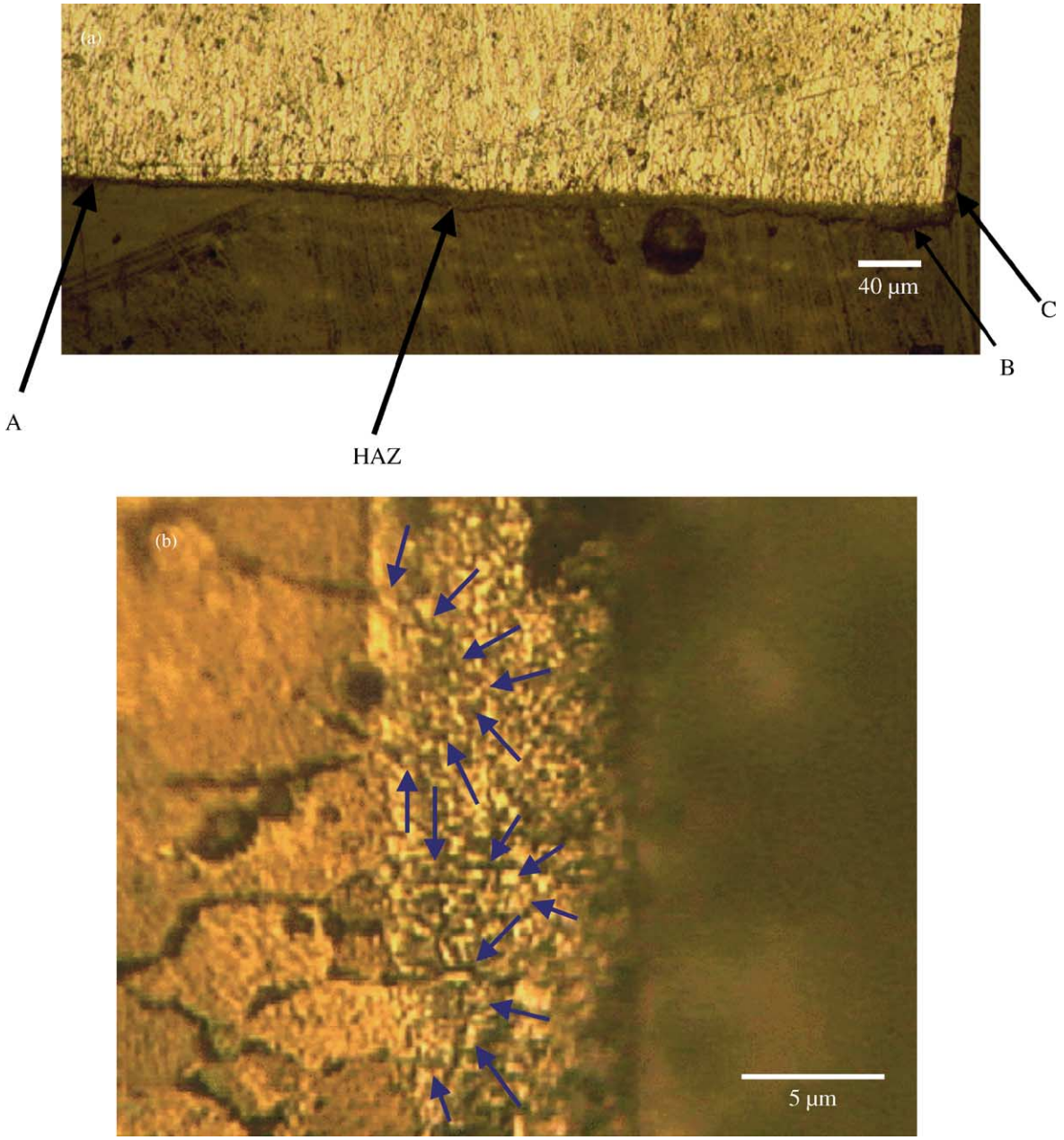

Fig. 2. Cross-section optical microscopy micrograph after Keller wet etching. (a) The HAZ depth variation can be observed as the laser beam cross the material from arrow A to B. Arrow C shows melted material that drips out of the material by the gas pressure. (b) Details of the HAZ at middle depth. Arrows indicate the "original" domains of the grains.

feature is peculiar for Al–Cu 2xxx alloy series. It induces the dripping region as a result of the high viscosity of the α-liquid mixture material that is pushed out by the gas pressure as shown in Fig. 3. Therefore, the darker superficial contrast corresponds to the region staying between 580 and 650 °C during the local laser cutting process. Note that difference in contrast is not related to significant changes in

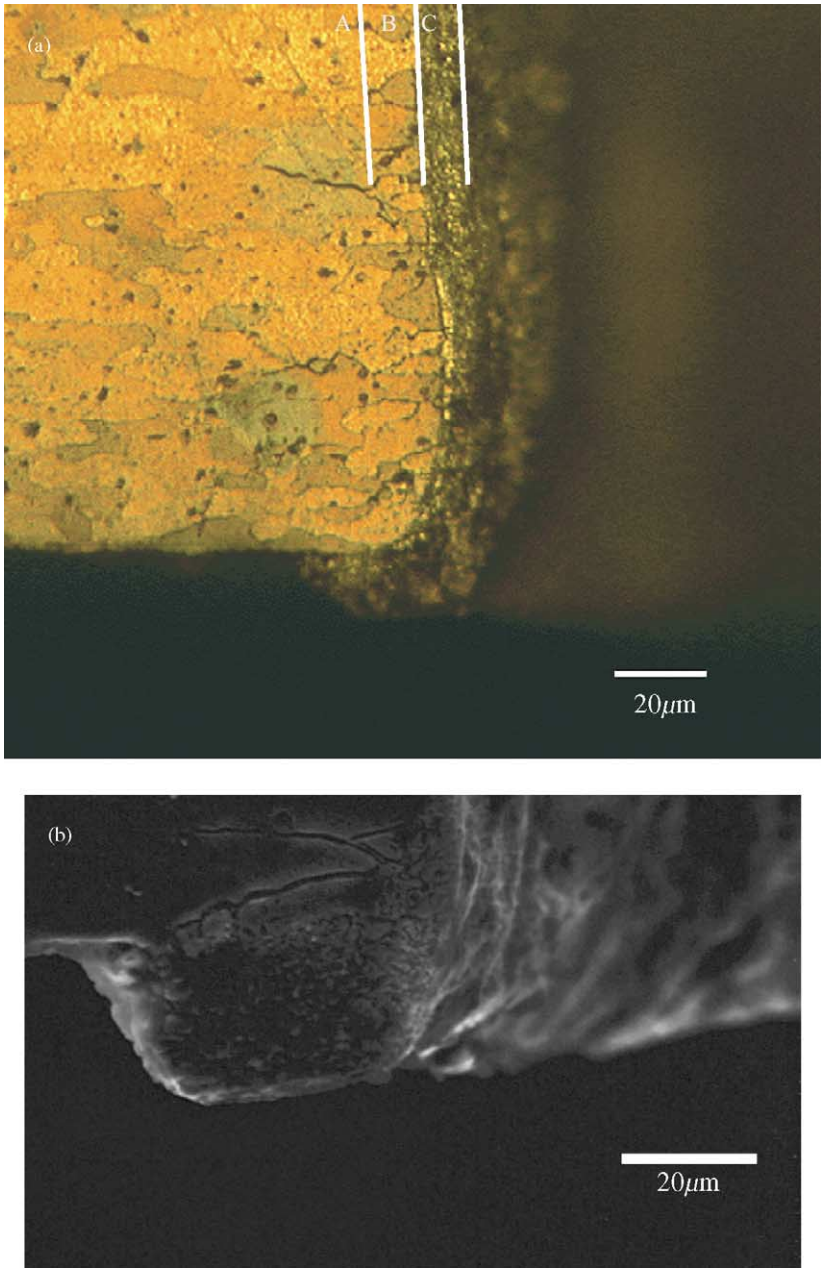

Fig. 3. Optical (a) and SEM (b) cross-section micrographs showing a detail of the dripped melted material pushed out by the gas during the laser process. In the SEM micrograph the defocused curvature of the laser machined hole and the roughness due to the solidification of partially melted material can be observed. In Fig. 3b three regions are marked by white lines. Region A corresponds to untreated material. The elongated grains result from lamination of the sheet before making test sample. In region B, those elongated grains are just cut. In region C, the other part of those grains suffer the laser base thermal treatment. Indeed they partially melt. The α-grains structure persists as indicate as indicate the Fig. 2b (see arrows). No significant compositional changes have been observed by SEM–EDX.

composition which is confirmed by SEM-EDX experiments.

Fig. 2b shows how grain size do not change vincinally to the laser process and how the grains are simply cut. The apendice at the bottom micrograph corresponds for Al–Cu (4% Cu), i.e. half way to the eutectic point. This is normally not observed for other Al alloys as the 6xxx or 7xxx series. Indeed, if the whole material directly melts the light absorption sharply increases and evaporation occurs in an easier way: less

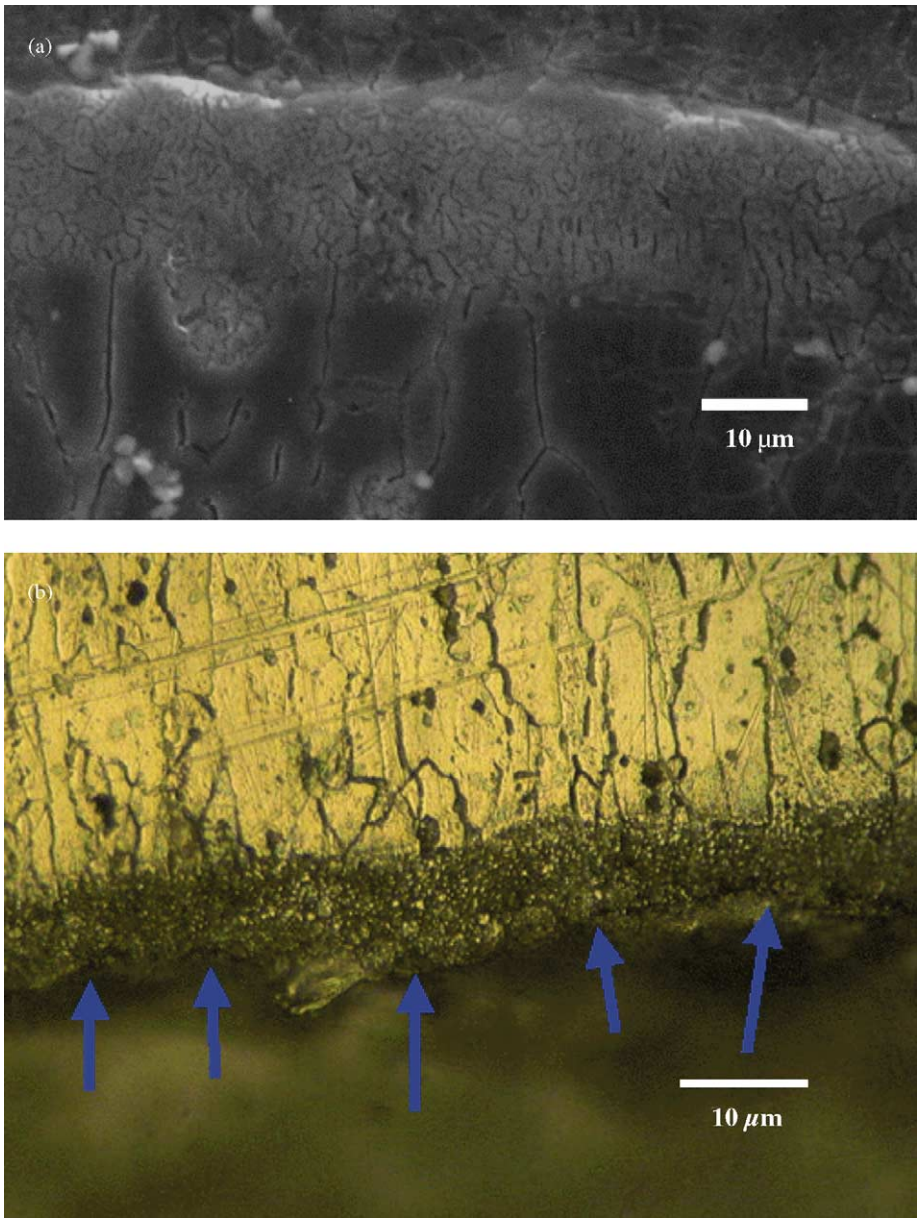

Fig. 4. Cross-section SEM micrographs showing three types of stress concentration defects: (i) superficial 1–2 μm thick cracks (see circles in (a)), (ii) roughness (see arrows in (b)), (iii) fringes induced during the laser beam displacements (c). Vertical arrow indicates the direction of the laser beam.

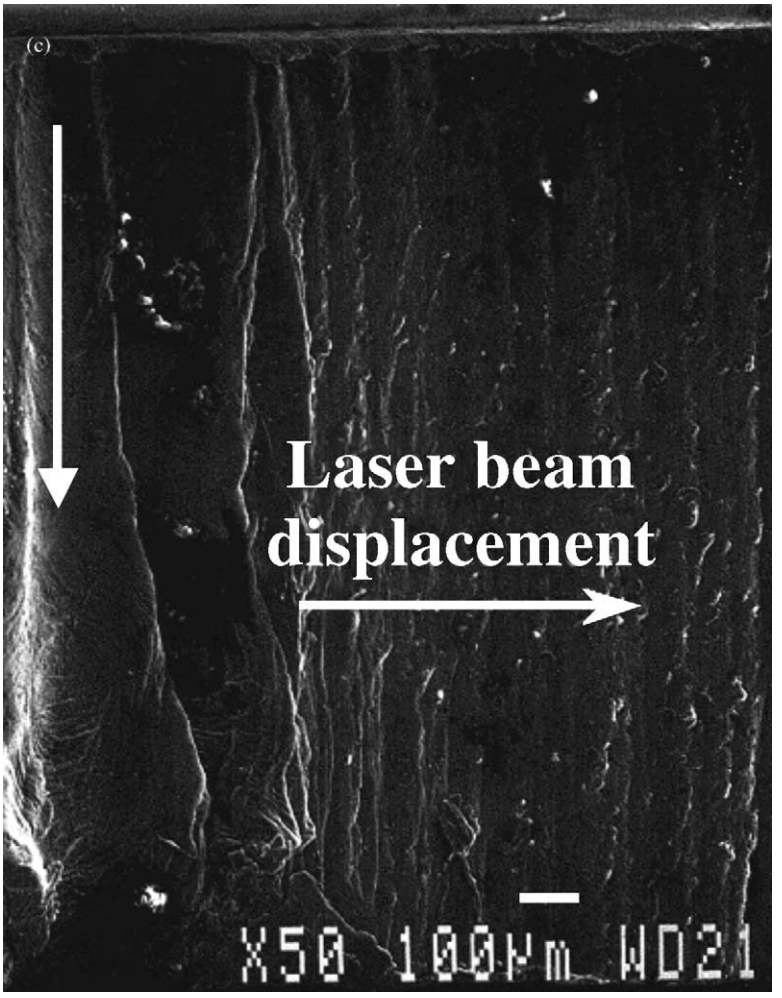

Fig. 4. (*Continued*).

wasting energy, less viscous material therefore much lower amount of dripped materials. This uncompleted melted material is shown to induce surface roughness as evidenced in Fig. 4b.

In Fig. 4, three types of possible stress concentration defects can be observed: superficial cracks, random roughness and macrofringes. The first seems to be due to the large temperature range of the α-liquid region of the Al–Cu phase diagram at 4% Cu (580–650 °C) and to mixed phase mechanical grain organization during solidification. As a result, microcracks are generated (see circles in Fig. 4a). The roughness is probably promoted by the high viscous material perturbed by the gas turbulence during the laser cutting. Therefore, the surface quality strongly changes compared to pure Al laser shock peening (LSP) where the surface is smoothed by the direct solid–liquid transition [5]. Here, much more viscous material is generated and high pressure gas flow modifies its surface topography. As a macroscopic result, the fringes shown in Fig. 4c are induced by these two factors. Indeed, fringes are not rigorously parallel to the laser beam. Their shape and rugosity indicate a N_2 gas flow induced phenomenon.

This rugosity (in this case the random roughness) should promote stress concentration. Indeed in Fig. 5

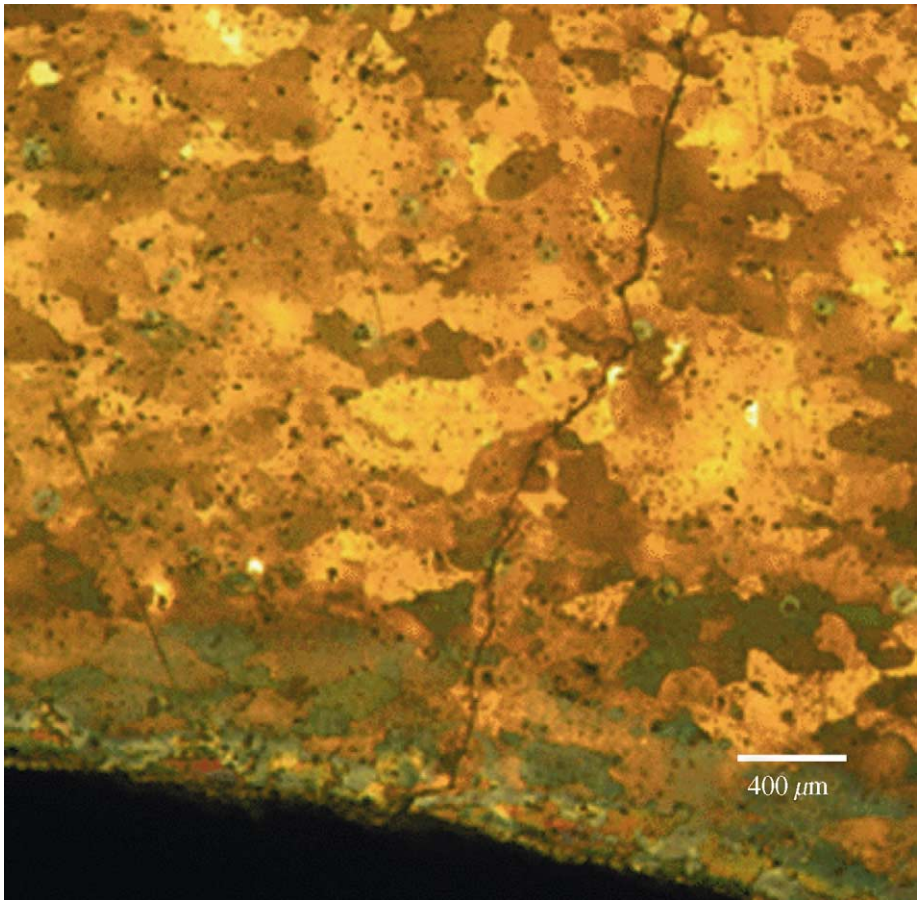

Fig. 5. Planar view optical micrograph after polishing and Keller wet etching of a fatigue crack generated at a stress concentration region.

fatigue crack generation is observed to be induced in such locations.

4. Conclusion

Optical and SEM studies of CO_2 laser machined Al 2024 sheets allow to understand the mechanisms generating the HAZ. Due to the large α-liquid region at 4% Cu of the Al–Cu phase diagram and to the low laser absorption factor of solid state Al at $\lambda = 10.2$ μm, the material first partially melts before evaporation/sublimation of the liquid-α material. Indeed, the absorption phases change from 1 to 8% during the phase transition promoting and immediate evaporation/sublimation of the partially melted material. On the other hand, the high pressure gas induces a dripping of that high viscous melted material and in this way degrades the surface quality of the laser machined material. This promotes a generation of high stress concentration regions that might affect its fatigue resistance. These features should be reduced either using a new Al aeronautic alloy such as 7475 or by using a higher power YAG source for the laser machining. However, 5 μm roughness is below aeronautic requirements.

References

[1] A. Corcoran, L. Sexton, B. Seaman, P. Ryan, G. Byrne, J. Mat. Proc. Techn., in press.

[2] H. Brücher, J.H. Schäfer, J. Uhlenbasch, J. Appl. Phys. 66 (1989) 1321.
[3] M.T. Jahn, J. Luo, J. Mater. Sci. 23 (1988) 4115.
[4] B.B. Verma, J.D. Atkinson, M. Kumar, Bull. Mater. Sci. 24 (2) (2001) 231.
[5] Z. Hong, Y. Chengye, Mat. Sci. Eng. A 257 (1998) 322.
[6] Y.K. Zhang, X.R. Zhang, X.D. Wang, S.Y. Zhang, L.Y. Gao, J.Z. Zhon, J.C. Yang, L. Cai, Mat. Sci. Eng. A 297 (2001) 138.
[7] J.H. Yang, Y.C. Her, M. Han, S. Klein, H. Naff, J.H. Schäfer, Mat. Sci. Eng. A 298 (2001) 296.
[8] J. Uhlenbasch, V. Bielesch, S. Klein, H. Naff, J.H. Schäfer, Appl. Surf. Sci. 106 (1996) 228.